Positron Emission Tomography - PET

Positron Emission Tomography

Positron Emission Tomography (PET): Coincidence detection of annihilation radiation from positron-emitting isotopes followed by tomographic reconstruction of 3-D activity distribution.

Some unique features of PET:

- Use of “electronic collimation” instead of lead collimation.
- High detection efficiency
- Uniform resolution
- Accurate attenuation correction
- “Absolute” Quantification
- Use of short-lived biologically active radio-pharmaceuticals:
  ^{11}C-glucose
  ^{13}N-ammonia
  ^{15}O-water
  ^{18}FDG
  ^{18}FDOPA

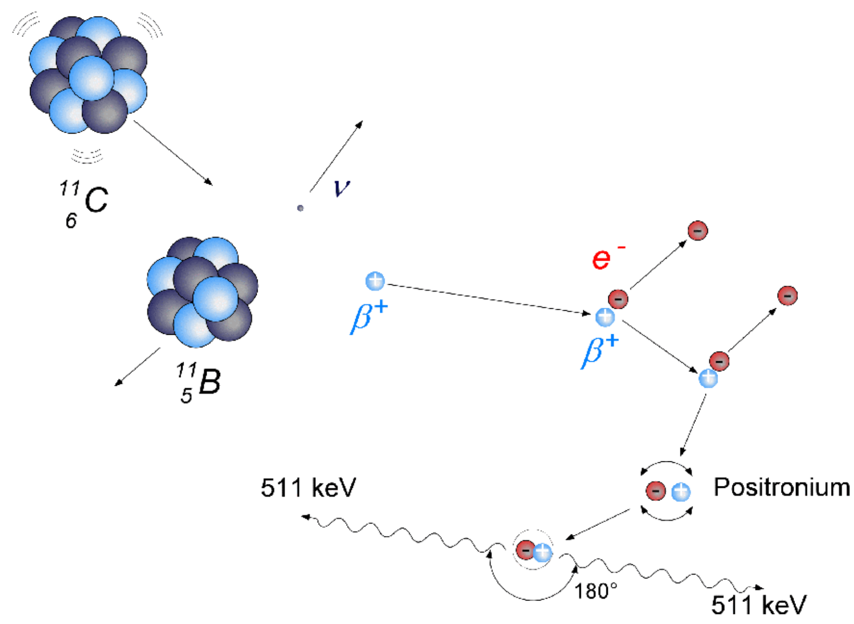

Coincidence Detection

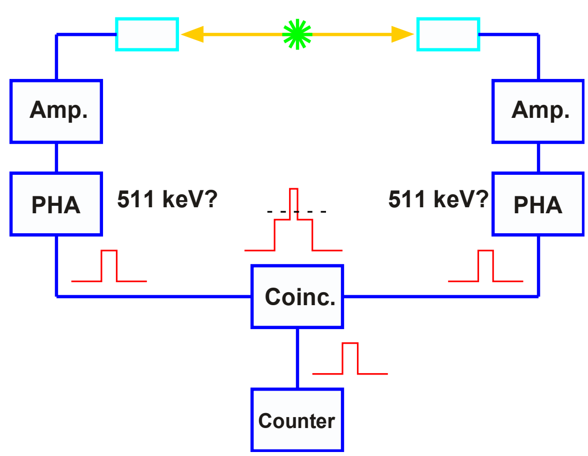

PET Gantry

ECAT HR+

PET Gantry

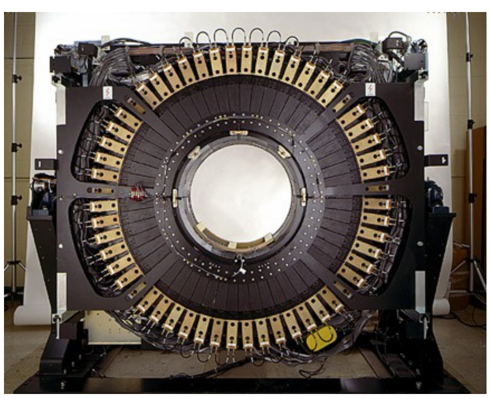

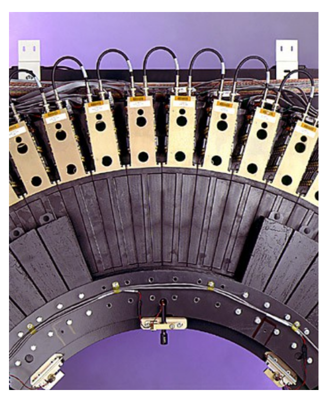

Siemens Hi-Rez / Biograph 16 Hi-Rez

Bernard Bendriem, Ph.D.
Vice-President, R&D
March 19, 2004

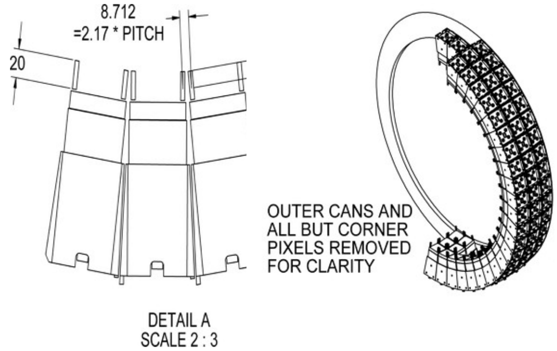

LSO 13x13 elements/block – 4x4x20mm^2 detector elements

Our Vision Changes Imaging

Coincidence Detection

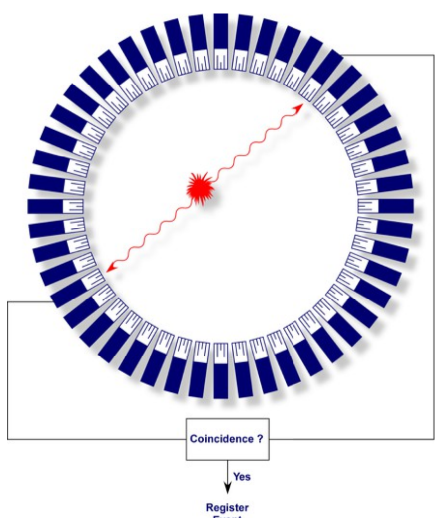

Coincidence Detection

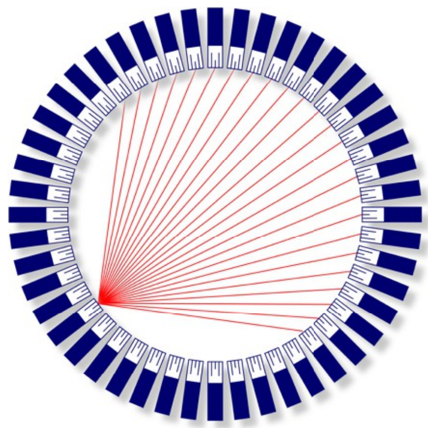

# of possible LORs: $N_{LOR} = \frac{N(N-1)}{2}$
N = number of detectors

Spatial Resolution

The spatial resolution in PET is primarily determined by:

- Detector size
- Physics of positron decay
- System geometry
- Detector material

Spatial Resolution

For a source placed at the midpoint between two scintillation detectors with a width w_d, the geometric line spread function has a triangular shape with a FWHM of w_d /2.

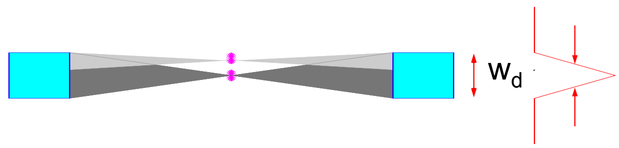

FWHM = $w_d/2$

Spatial Resolution -Tangential

For sources located between the midpoint and the detector surface the LSF will have a trapezoidal shape with width varying from w_d /2 (at the center) and w_d at the detector surface.

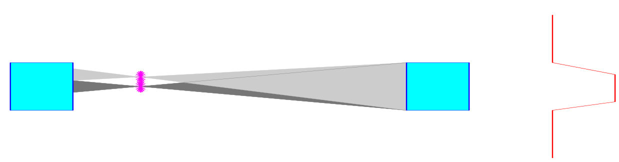

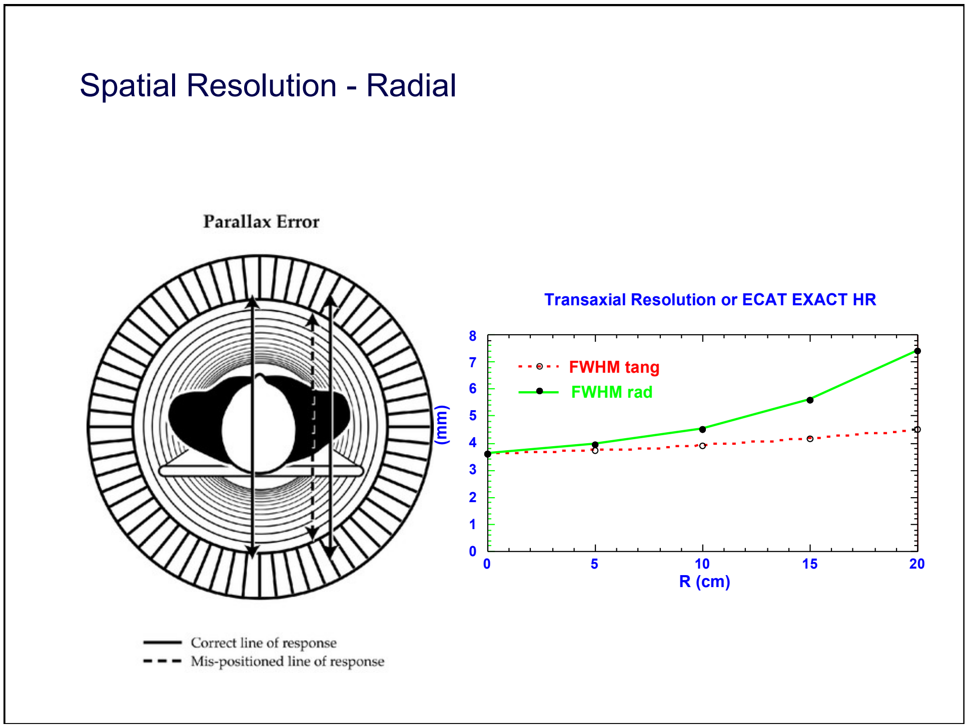
Spatial Resolution - Radial
Parallax Error
Correct line of response
Mis-positioned line of response
Transaxial Resolution or ECAT EXACT HR
FWHM tang
FWHM rad
(mm)
R (cm)
0 5 10 15 20
0 1 2 3 4 5 6 7 8

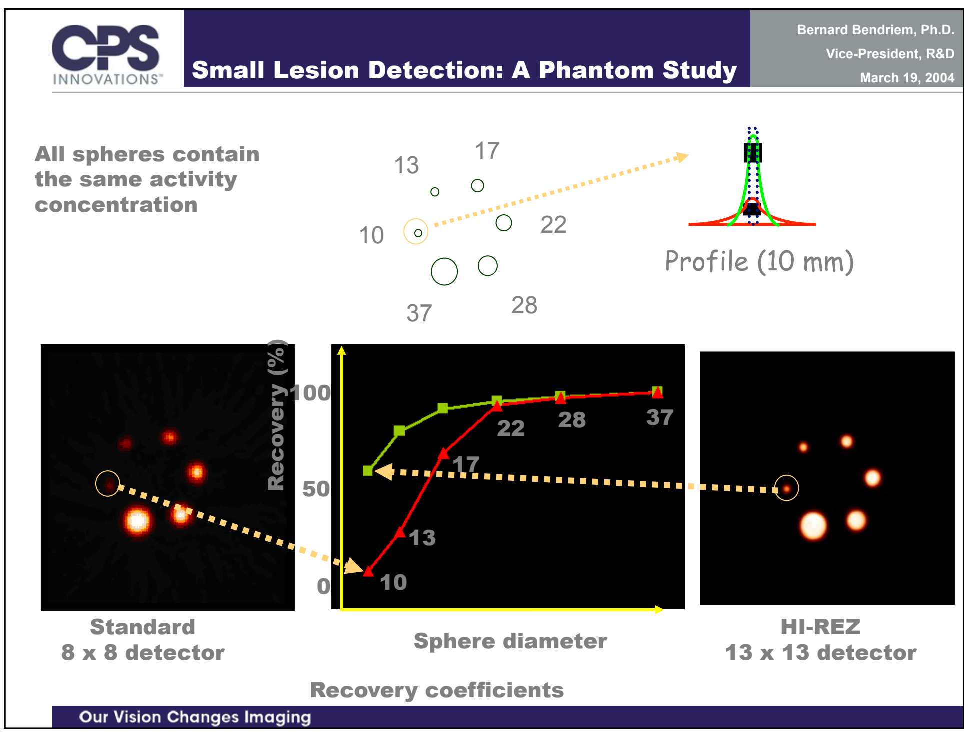
CPS INNOVATIONS
Small Lesion Detection: A Phantom Study
Bernard Bendriem, Ph.D.
Vice-President, R&D
March 19, 2004
All spheres contain the same activity concentration
10 13 17 22 28 37
Profile (10 mm)
Recovery (%)
100
50
0
10 13 17 22 28 37
Standard
8 x 8 detector
Sphere diameter
HI-REZ
13 x 13 detector
Recovery coefficients
Our Vision Changes Imaging

Spatial Resolution

Although the most energetic positrons can travel several mm before annihilating, only a few of these are emitted.

The average positron energy emitted is approximately 1/3-1/2 of the maximum energy.

The total path length the positrons travel is not along a straight path. Through inelastic interactions with electrons in the positrons path is deflected. The distance from the mother nucleus is therefore much shorter.

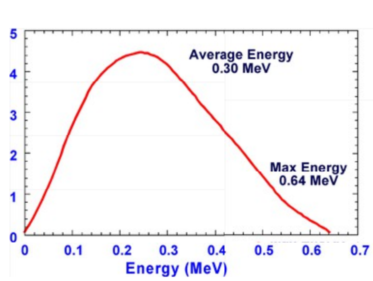

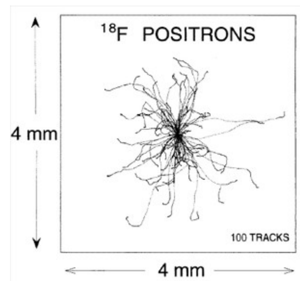

Positron Range

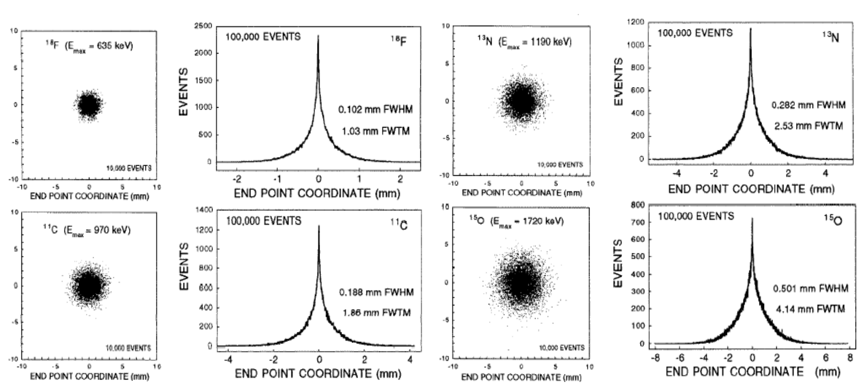

From Levin & Hoffman PMB 44, 1999

Positron Range

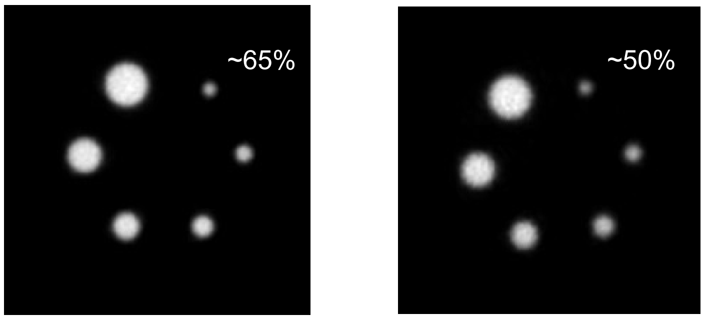

^{18}F
635 keV

^{124}I
1.53 & 2.14 MeV

Non-colinearity

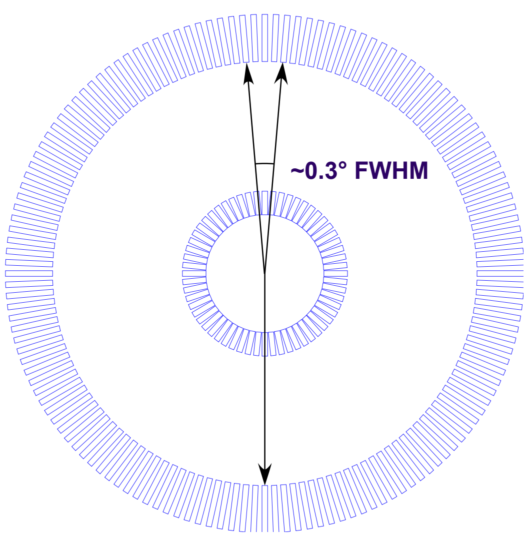

100 cm Ø ~ 2.5 mm FWHM

15 cm Ø ~ 0.3 mm FWHM

Spatial Resolution

The measured resolution (intrinsic resolution) of the system is a convolution of the various resolution components.

If the different resolution components are assumed to be Gaussian in shape and are described by a FWHM then the combined resolution is the squared sum of the individual resolution components:

$$FWHM_{total} = \sqrt{FWHM^2_{detector} + FWHM^2_{positron} + FWHM^2_{angulation}}$$

3D Acquisition PET

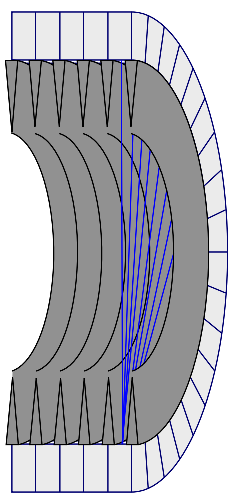

2D Acquisition PET

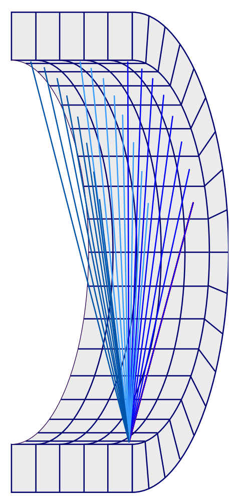

3D Acquisition PET

3D vs. 2D PET

The main advantage of the 3-D acquisition in PET is an improved sensitivity of ~5-7 times the 2-D sensitivity.

The drawback is that the scatter fraction increases by a factor of 3.

Non-uniform axial sensitivity

Higher Randoms Rates → Increased Noise (offsets sensitivity gain)

Dead-time problems when using slow detectors

Image reconstruction is more complex

More data

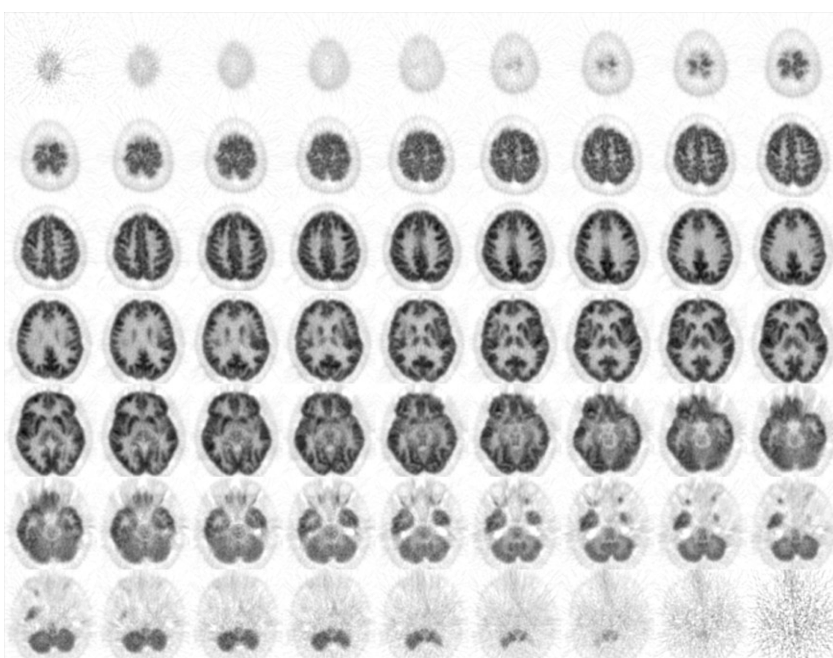

Coincidence Detection

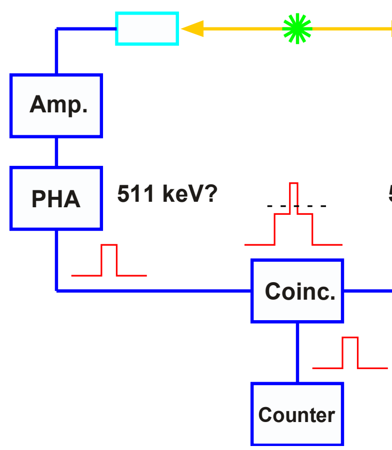

Timing Resolution

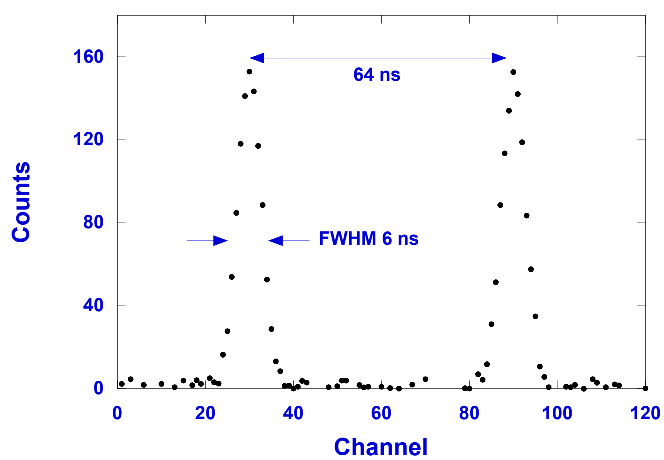

Timing spectrum showing the PHA trigger time variation for a pair of BGO detectors in coincidence. The two peaks corresponds to two separate measurements where an additional delay of 64 ns of the stop pulse for channel-to-time calibration.

Coincidence Detection

All coincidence detection systems have a finite time resolution

BGO	~6 ns FWHM
NaI	~4 ns FWHM
GSO	~2 ns FWHM
LSO	~0.5 ns FWHM

Coincidence Detection

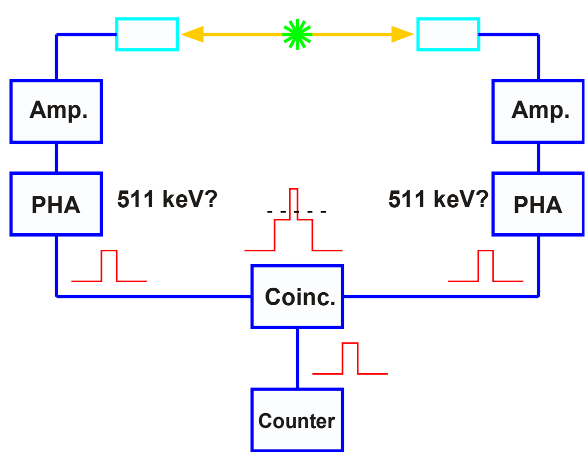

Random Coincidences

Because of the finite width of the logic pulses that are fed into the coincidence circuit, there is a probability for random or accidental coincidences between unrelated events.

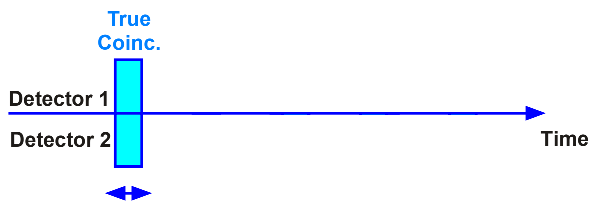

Random Coincidences

If N_1 and N_2 are the individual average count rates of detector 1 and 2, respectively, then it can be shown that the random coincidence rate for the pair of detectors is:

$$N_R = 2\tau\, N_1 N_2$$

Where 2τ is the coincidence window (or τ is the width of the singles pulses)

Event Types

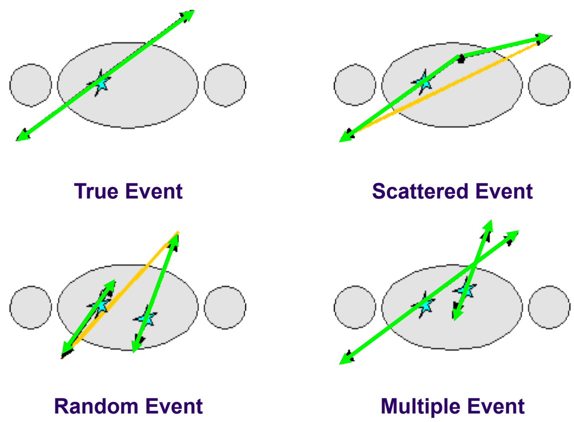

Signal-to-Noise

True Coincidences

~ Activity

Good events!

$$S/N \sim \frac{T}{\sqrt{T}}$$

Signal-to-Noise

Random Coincidences

- ~ Activity^2
- Can be accurately corrected for
- Correction increases image noise
- Detector material dependent

$$S/N \sim \frac{T}{\sqrt{T+2R}}$$

Signal-to-Noise

Scattered Coincidences

- ~ Activity
- Reduces Image Contrast
- Requires correction
- Analytical estimation
- Correction increases image noise

$$S/N \sim \frac{T}{\sqrt{T+S+2R}}$$

Signal-to-Noise

Multiple Coincidences:

- ~ Activity^3
- Never saved
- Source of Dead time

Improvements in PET Image Quality

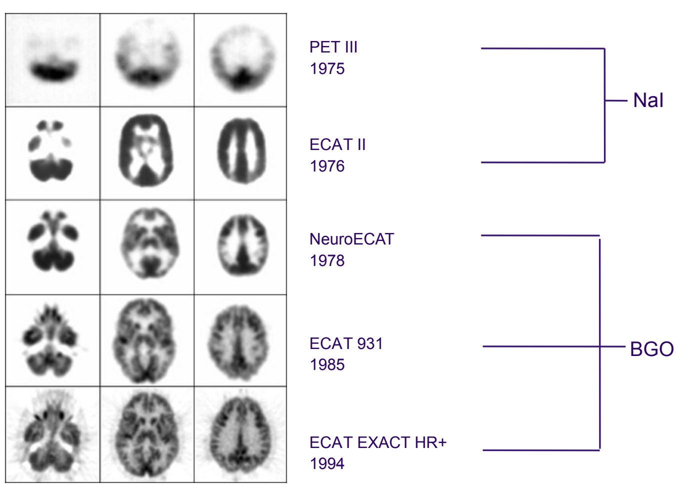

CTI/Siemens

PET Detectors

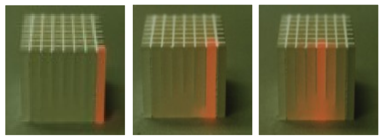

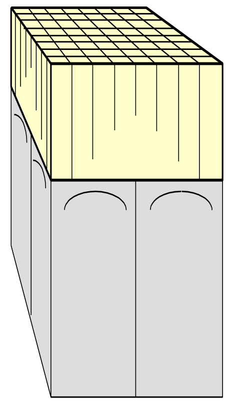

Most modern PET system use a different detector technology where a large number of scintillation crystals are coupled to a smaller number of PMTs.

In the block detector, a matrix of cuts are made into a solid block of scintillator material to define the detector elements.

The depth of the cuts are adjusted to direct the light to the PMTs.

The light produced in each crystal, will produce a unique combination of signals in the PMTs, which will allow the detector to be identified.

CPS INNOVATIONS

The Technology : HiRez

Bernard Bendriem, Ph.D.
Vice-President, R&D
March 19, 2004

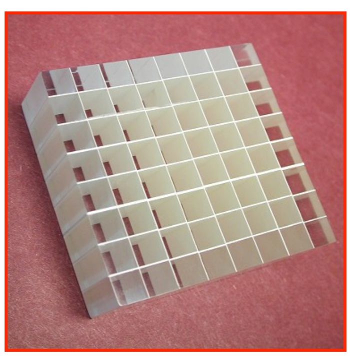

Standard Detector
6.4 mm x 6.4 mm
64 crystals/block
144 blocks/scanner
9216 crystals/scanner
3.4 mm slice width
47 slices

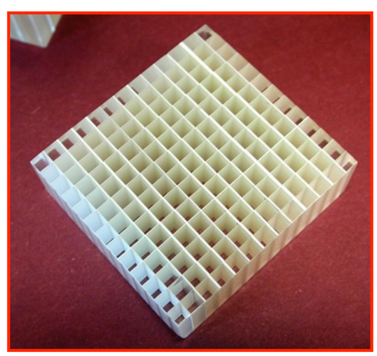

HI-REZ Detector
4.0 mm x 4.0 mm
169 crystals/block
144 blocks/scanner
24336 crystals/scanner
2 mm slice width
81 slices

Our Vision Changes Imaging

Scintillator Materials

	NaI (Tl)	BGO	GSO	LSO	LYSO	$LaBr_3$
Density [g/ml]	3.67	7.13	6.71	7.35	7.1	5.29
$1/\mu$ [cm]	2.88	1.05	1.43	1.16	1.2	~2
Index of Refraction	1.85	2.15	1.85	1.82	1.81	1.9
Hygroscopic	Yes	No	No	No	No	Yes
Rugged	No	Yes	No	Yes	Yes	Yes
Peak Emission [nm]	410	480	430	420	420	380
Decay Constant [ns]	230	300	60	40	41	25
Light Output	100	15	35	75	75	>100
Energy Resolution	7.8	20	8.9	<9	11	7.5

CPS INNOVATIONS™

Our Vision
Changes Imaging

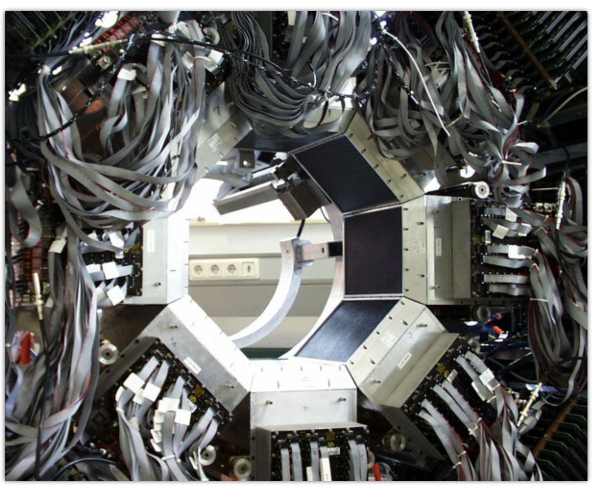

HRRT
CPS Innovations

56

CPS INNOVATIONS

Our Vision
Changes Imaging

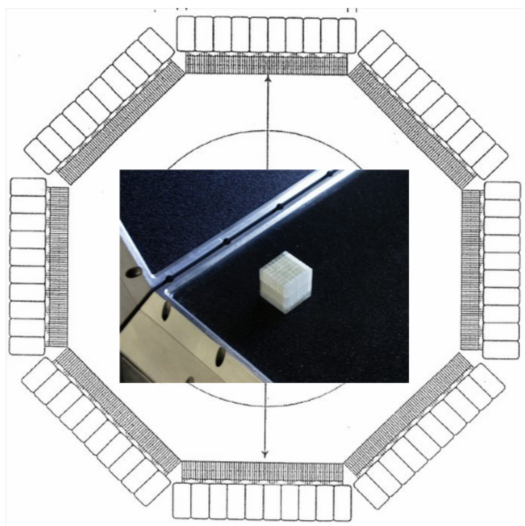

HRRT
CPS Innovations

57

Improvements in PET Image Quality

LSO
ECAT HRRT

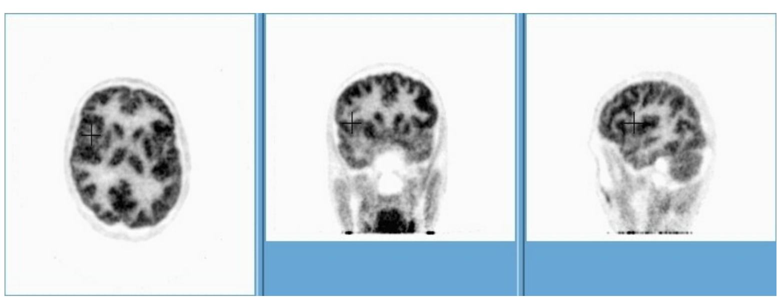

CTI/Siemens

Corrections in PET

In most nuclear medicine procedures, the goal is to produce an image in which the gray scale or count density is directly proportional to the regional isotope concentration.

In order to achieve this in PET it is necessary to apply a number of corrections:

- Attenuation of photons in tissue
- Non-uniform response of detector elements
- Random coincidence events
- Detection of scattered events
- Loss of counts at high count rates - dead-time
- Isotope decay
- Absolute Calibration & cross calibration with other instruments

How accurate these corrections are will have a direct impact on the quantitative measurement.

Attenuation Correction

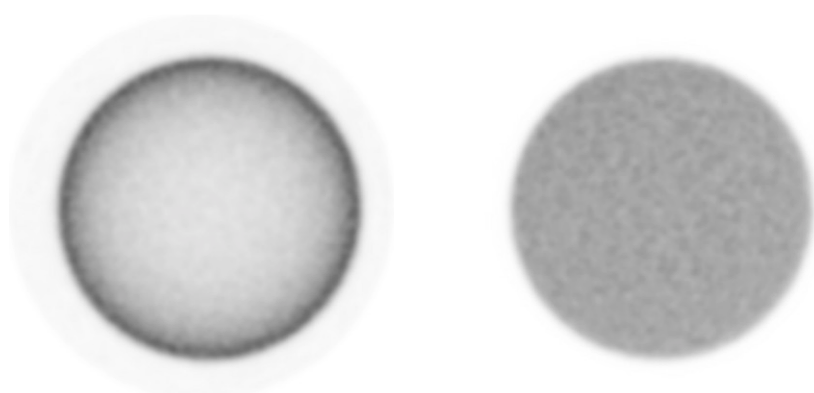

Attenuation Correction

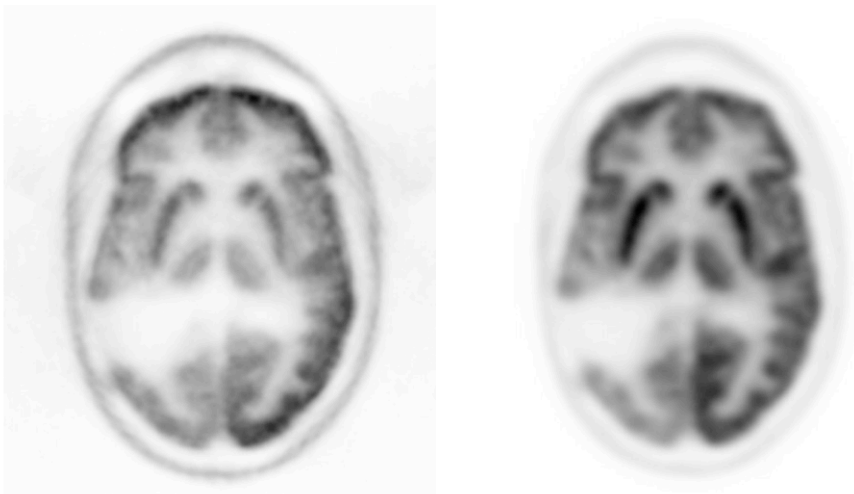

Attenuation Correction

In PET imaging of the brain, the shape of the head can be approximated with an ellipse. The dimensions of the fitted ellipse can be estimated by first reconstructing the data without attenuation correction. Then an ellipse is drawn onto the image from which the attenuation correction can be derived. The attenuation correction is the applied to the data and the image is reconstructed again.

This method can be fairly time consuming, especially on system producing a large number of transaxial slices.

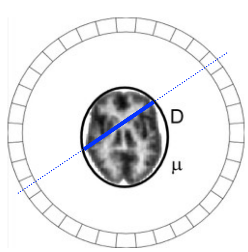

Atten. Corr. = $e^{\mu D}$

Attenuation Correction

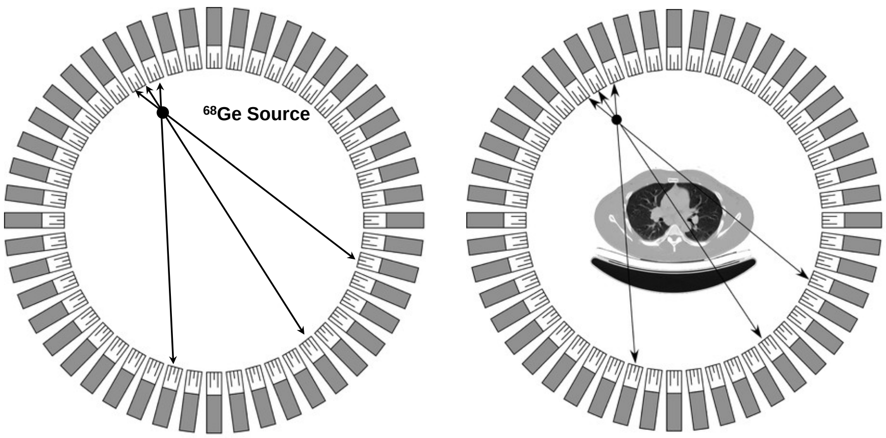

Blank Scan

Transmission Scan

Without Image Segmentation

With Image Segmentation

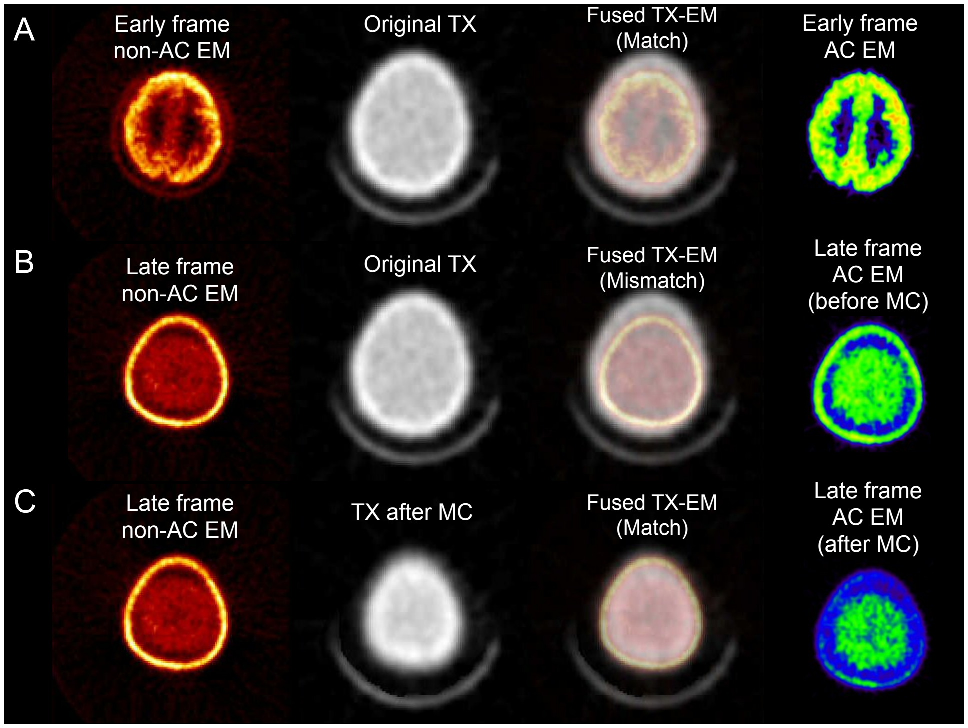

The use of X-ray CT for Attenuation Correction of PET Data

Thomas Beyer, Paul E. Kinahan, David W. Townsend, and Donald Sashin
Department of Radiology, University of Pittsburgh, Pittsburgh, PA 15213-2582

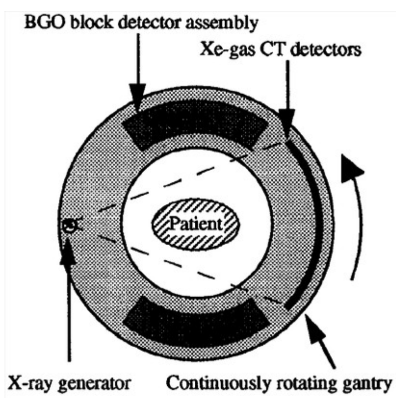

Figure 1. Outline of proposed PET/CT scanner.

PET/CT

GE

Philips

Siemens

x 0.495

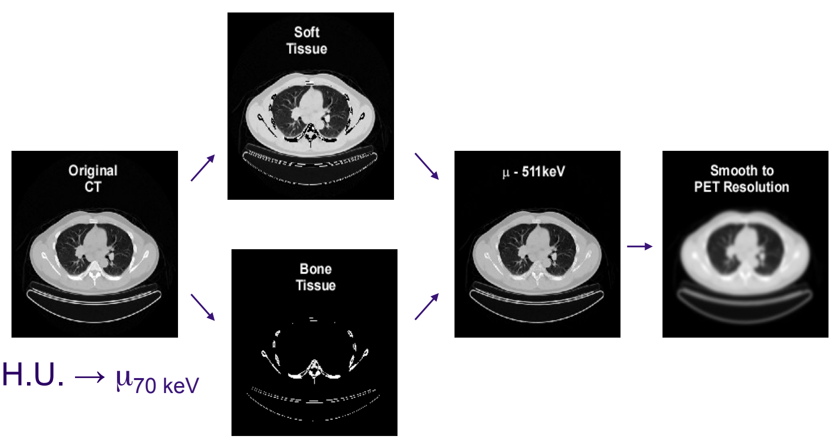

H.U. → $\mu_{70\ keV}$

x 0.406

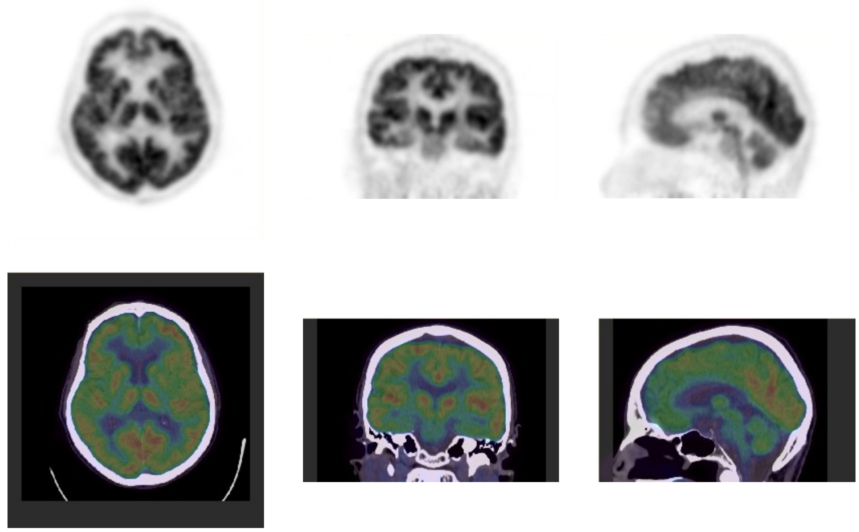

Time-of-flight PET

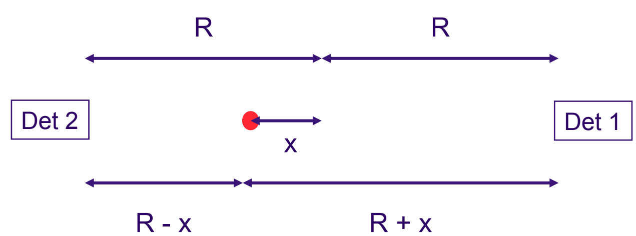

$$s = v \cdot t$$
$$R + x = vt_1$$
$$R - x = vt_2$$
$$2x = v(t_2 - t_1) \Rightarrow x = {c\Delta t}/{2}$$

Time-of-flight PET

For ideal detectors, TOF would eliminate the need for image reconstruction, since the measurement would allow each event to be accurately positioned in space.

All detectors have a finite time resolution, or uncertainty in timing. This translates to an uncertainty in positioning.

BGO ~ 5 ns	75 cm
NaI ~ 1.5 ns	22.5 cm
CsF, $LaBr_3$ ~ 0.45 ns	6.7 cm
BaF_2, LSO, LYSO ~ 0.3 ns	4.5 cm

Time-of-flight PET

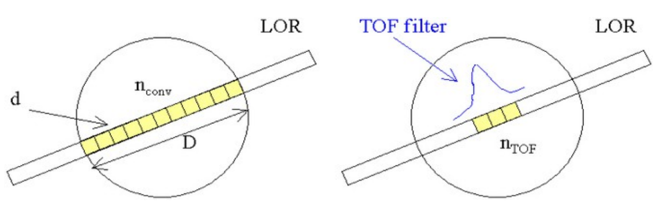

Figure 1. Image elements contributing to a LOR, for conventional PET (left) and TOF PET (right).

Time-of-flight PET

Even with a finite time resolution, using the TOF information an improvement in signal-to-noise ratio (S/N) can be achieved:

$$SNR_{TOF} \cong \sqrt{\frac{D}{\Delta x}} SNR_{conv.} = \sqrt{\frac{2D}{c\Delta t}} SNR_{conv.}$$

PHILIPS

Time-of-Flight vs. Conventional PET

Better information sent to reconstruction

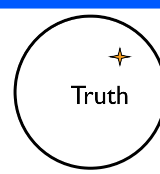

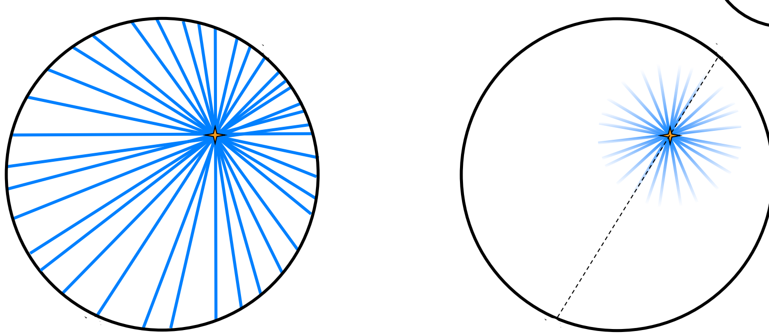

Conventional PET Image Formation

Time-of-Flight Image Formation

More precise localization of annihilation event improves image quality

Time-of-flight PET - 1980's

Problems with TOF in the 80's
Poor detection efficiency of available scintillators

TOF Gain did not offset the poor efficiency

To improve the efficiency, large detector modules were used

A more significant gain in S/N could be achieved by using high resolution detectors and conventional detection methods (Phelps, Hoffman, Huang, 1982).

Time-of-flight PET - 2006

Scintillators:
CsF, BaF_2 → LSO, LYSO - *fast, high light, and dense*

Detectors/PMTs:
1:1 coupling → 100:1 crystal encoding - *spatial resolution*

Geometry:
2D (septa) → 3D with large axial FOV - *sensitivity*

Reconstruction:
Analytic (FBP) → iterative (list-mode) - *system modeling*

Electronics:
Accurate and stable

Can we see TOF improvement?

non TOF | TOF

5 min

3 min

1 min

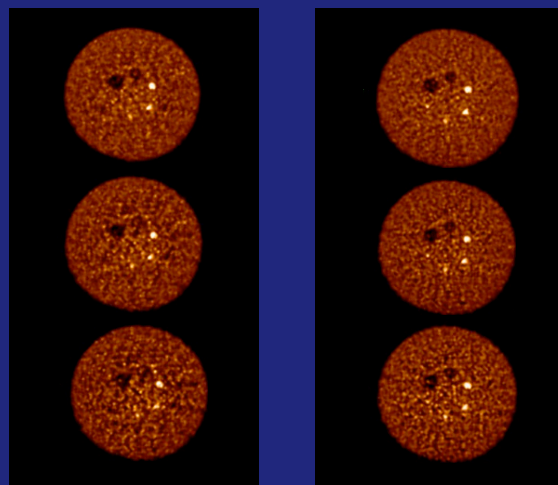

6-to-1 contrast; 35-cm phantom

J. Karp, U of Penn

Noticeable improvement with TOF with large size phantom

Gemini TF - patient study

Rectal carcinoma metastases in mesentery and bilateral iliac chains

114 kg; BMI = 38.1
12 mCi; 2 hr post-inj
3min/bed

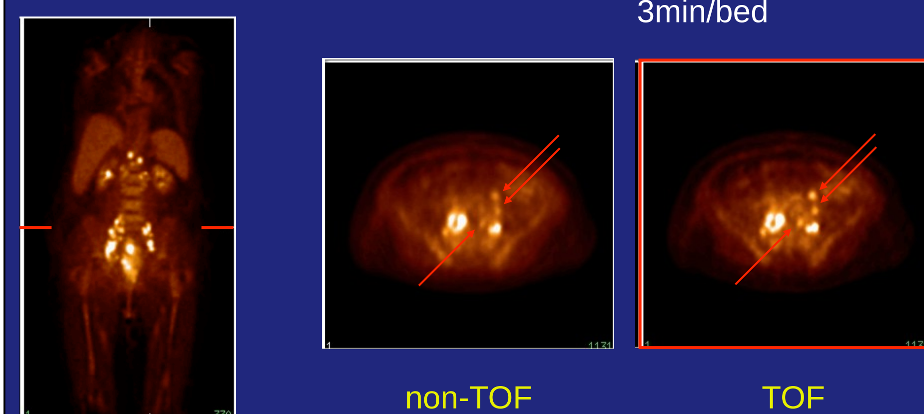

non-TOF

TOF

J. Karp, U of Penn

Lesion contrast (SUV) improves with TOF reconstruction

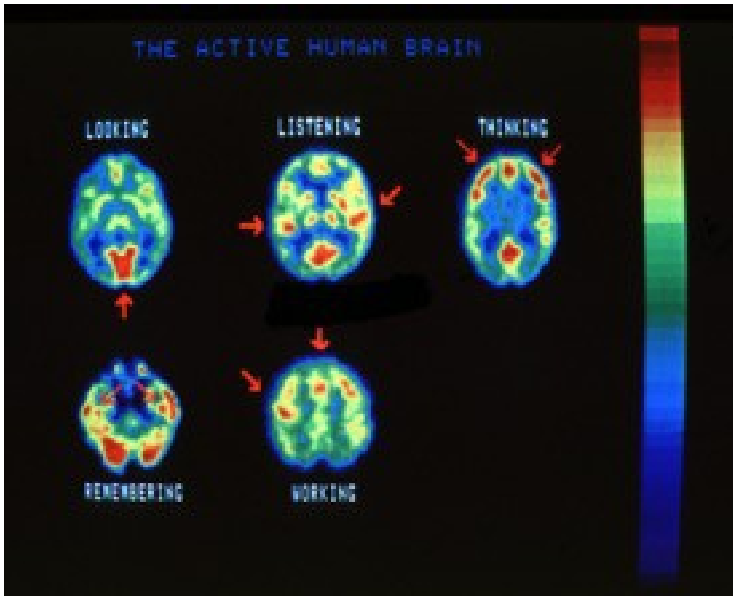

ME Phelps et. al.

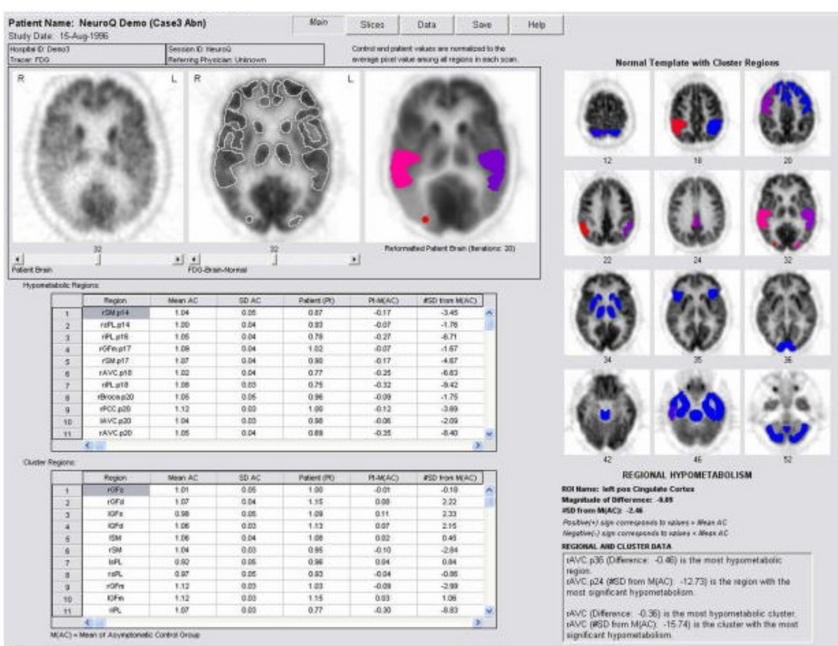

DH Silverman et. al.

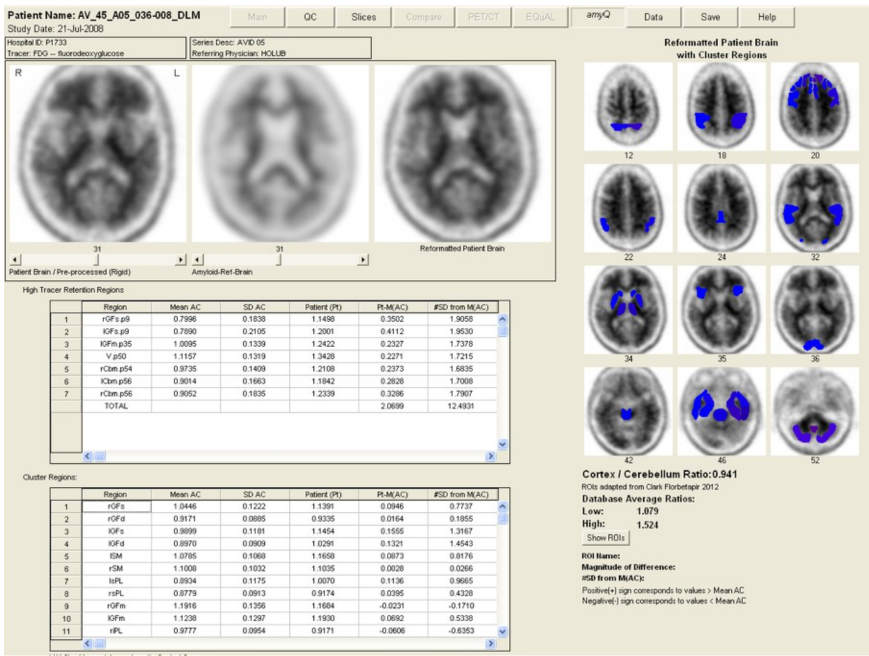

DH Silverman et. al.

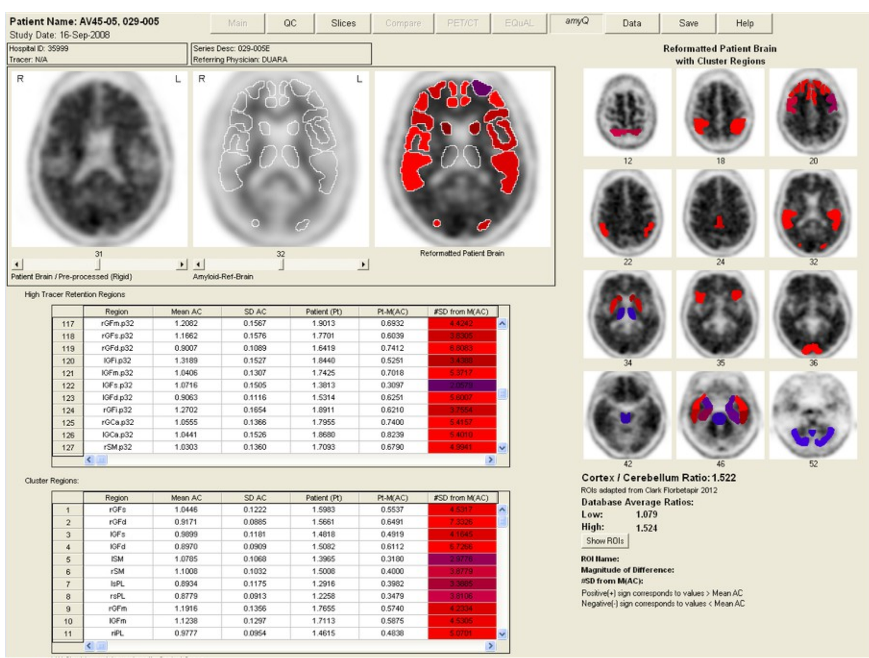

DH Silverman et. al.

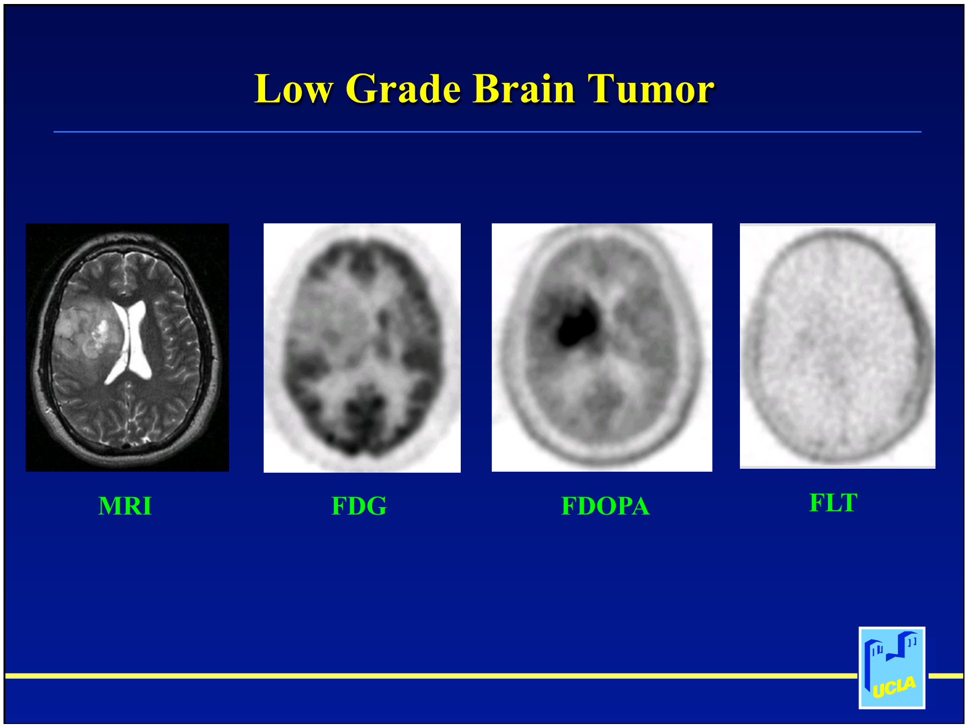
Low Grade Brain Tumor
MRI
FDG
FDOPA
FLT
UCLA

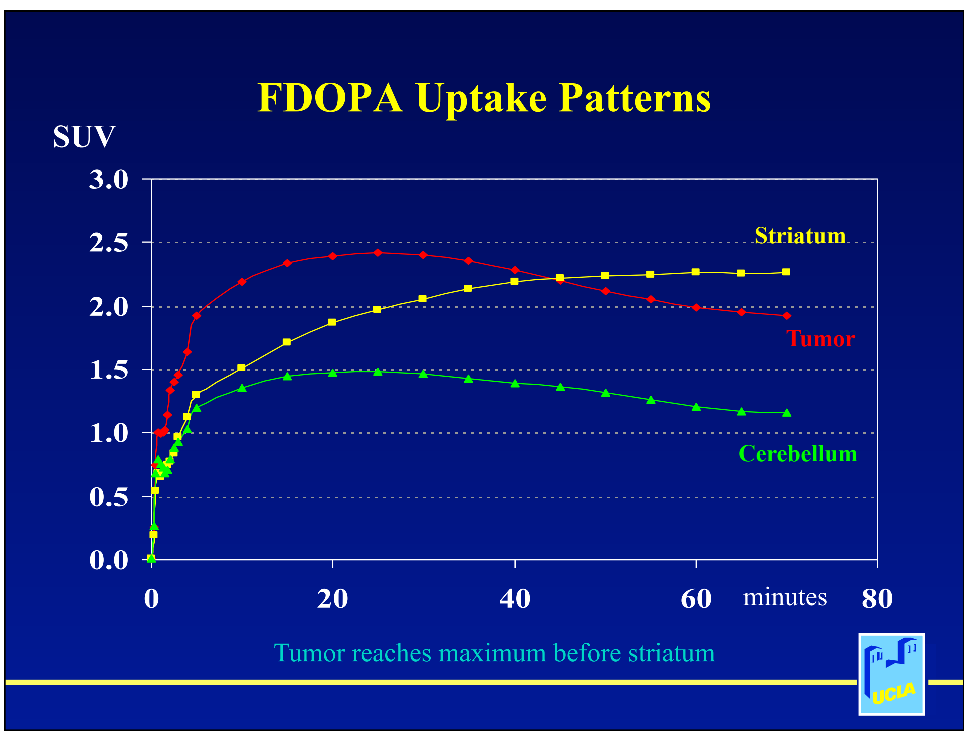
FDOPA Uptake Patterns
SUV
3.0
2.5
2.0
1.5
1.0
0.5
0.0
0
20
40
60
minutes
80
Striatum
Tumor
Cerebellum
Tumor reaches maximum before striatum
UCLA

Integrated PET/MRI System

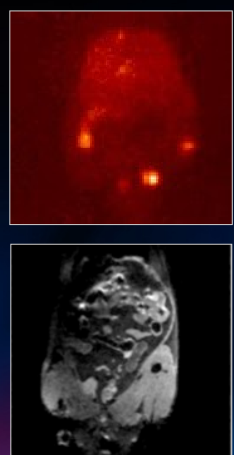

Images courtesy Bernd Pichler

Opportunities:

- direct and accurate registration of molecular PET signal with high resolution anatomy
  - Anatomically guided analysis of PET data
  - Improved quantification of PET data
  - Good soft tissue contrast, no additional radiation dose
- time correlation of PET and MRI or MRS signal
  - Interventional, therapeutic studies
  - Dual-labeled agents (^{64}Cu, Gd)

UCDAVIS UNIVERSITY OF CALIFORNIA cmg

Positrons in Magnetic Field

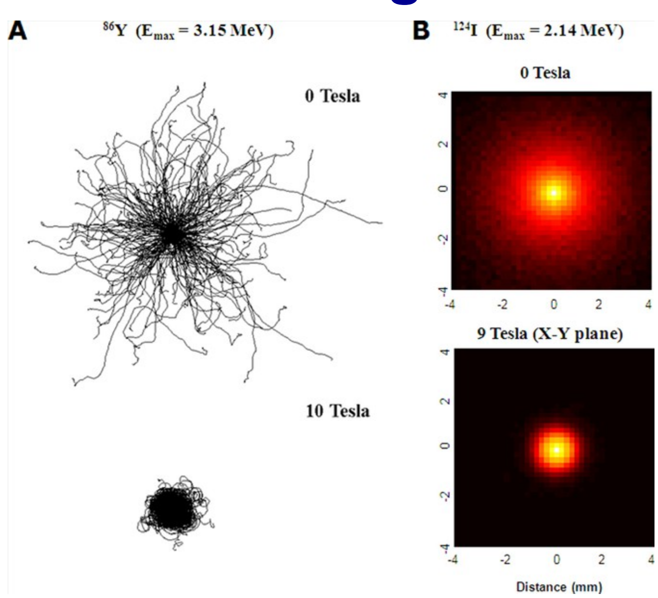

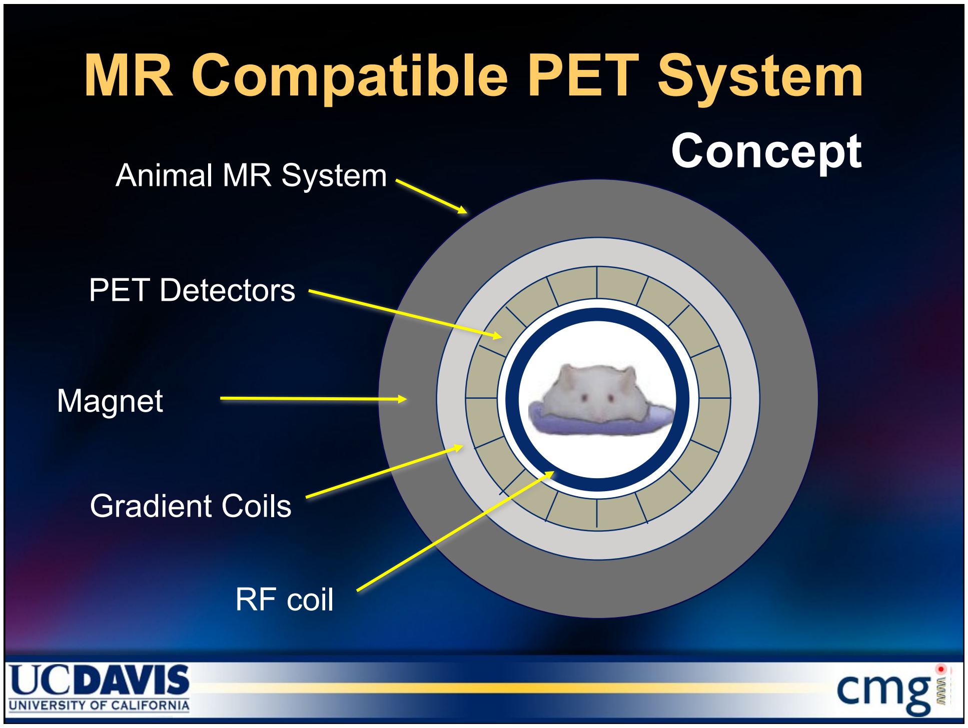
MR Compatible PET System
Concept
Animal MR System
PET Detectors
Magnet
Gradient Coils
RF coil
UCDAVIS
UNIVERSITY OF CALIFORNIA
cmgi

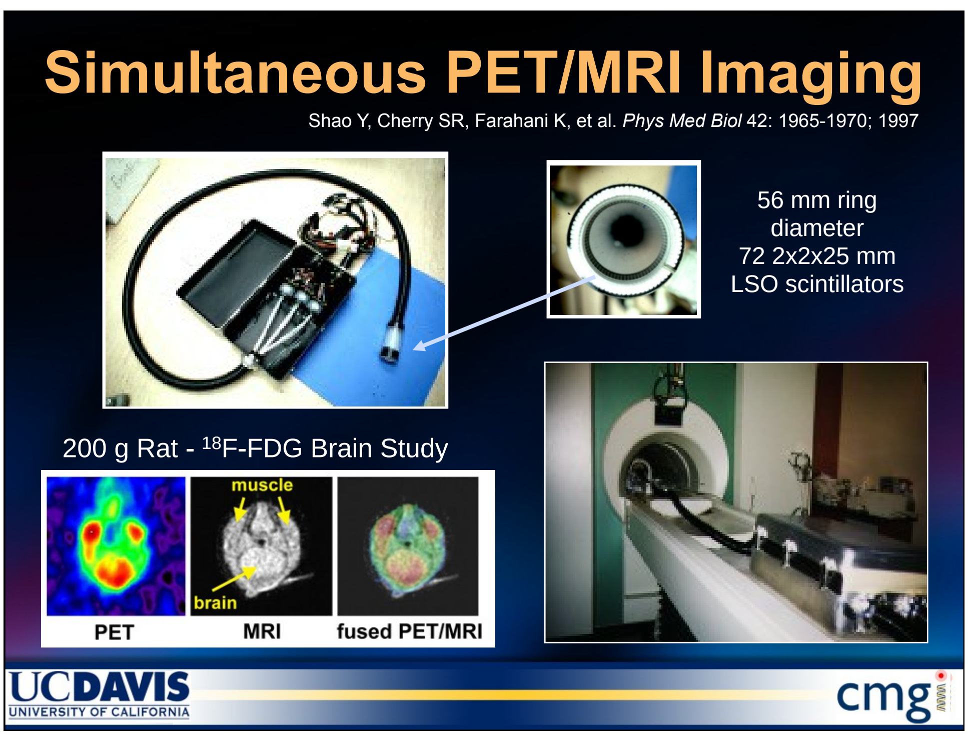
Simultaneous PET/MRI Imaging
Shao Y, Cherry SR, Farahani K, et al. *Phys Med Biol* 42: 1965-1970; 1997
56 mm ring diameter
72 2x2x25 mm LSO scintillators
200 g Rat - ^{18}F-FDG Brain Study
muscle
brain
PET
MRI
fused PET/MRI
UCDAVIS
UNIVERSITY OF CALIFORNIA
cmgi

Challenges in Combining PET and MR imaging

PET Detectors affected by:
Static magnetic field
Rapidly changing gradient field
Radiofrequency signals

MR affected by
PET detectors and electronics

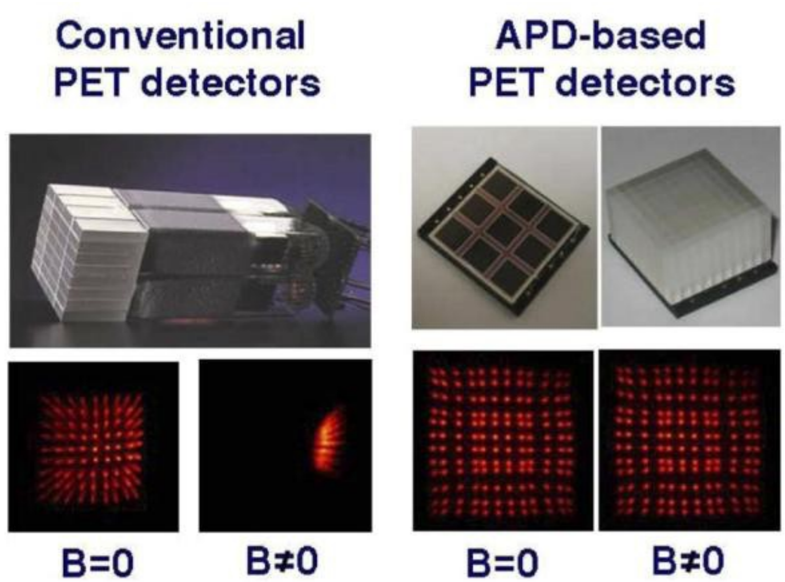

B. Pichler et. al., 2008

Solutions for combining PET-MR

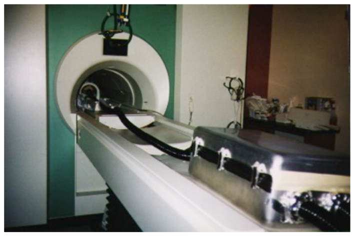

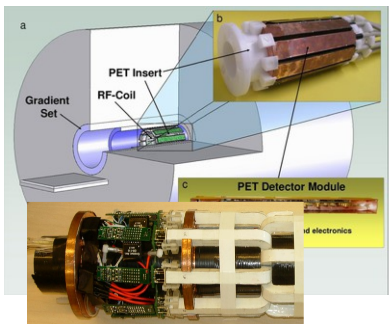

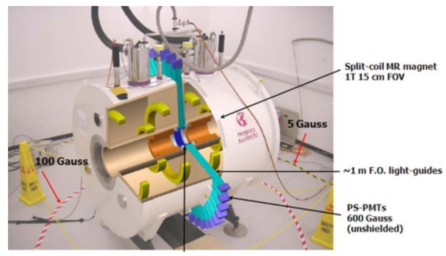

MR-Compatible PET Detector Module

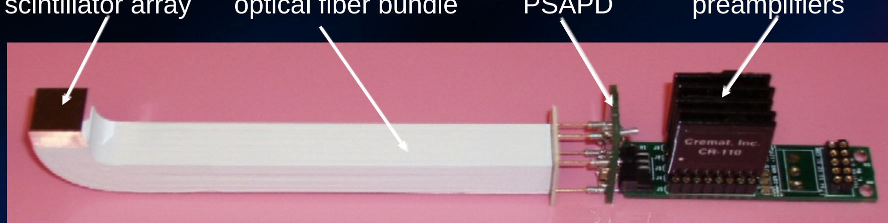

UCDAVIS
UNIVERSITY OF CALIFORNIA

cmg

PMT vs. APD/SiPM

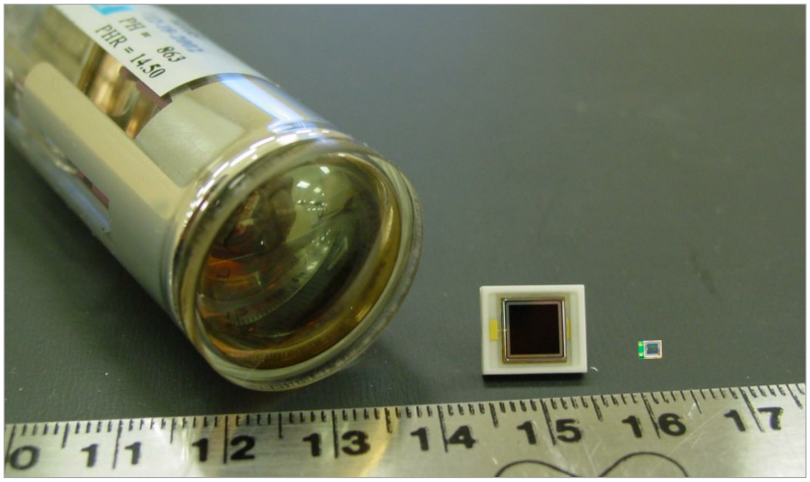

PET Insert

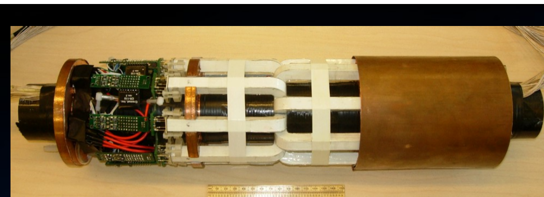

preamplifiers PSAPDs optical fibers scintillator ring

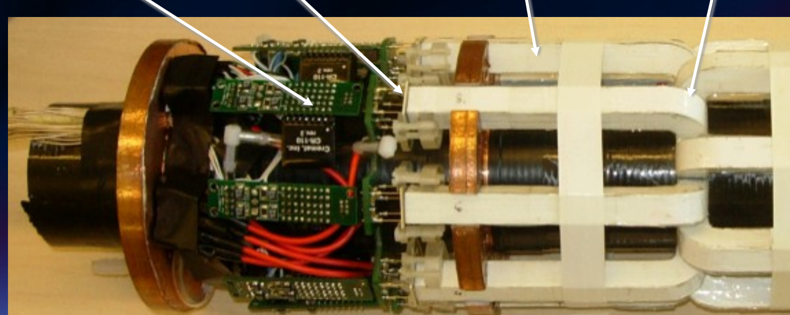

UCDAVIS
UNIVERSITY OF CALIFORNIA

cmgi

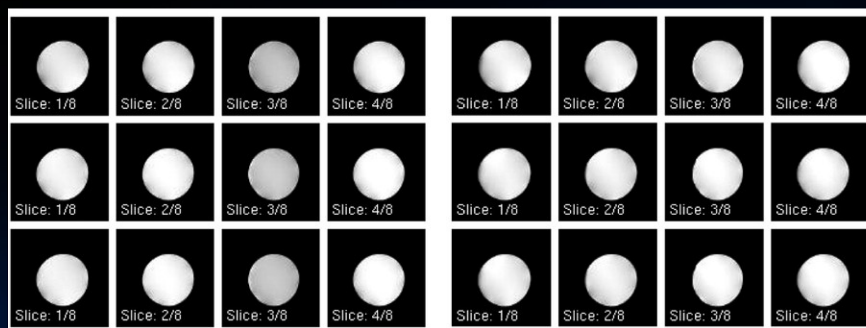

MR phantom images: GE (left) and SE (right) sequences of a gadopentetate dimeglumine/H2O phantom (T1 = 250 ms) without PET insert (first row) and with PET insert unpowered (second row) and powered (third row).
Catana et.al., JNM 47 (12), 2006

UCDAVIS
UNIVERSITY OF CALIFORNIA
cmg

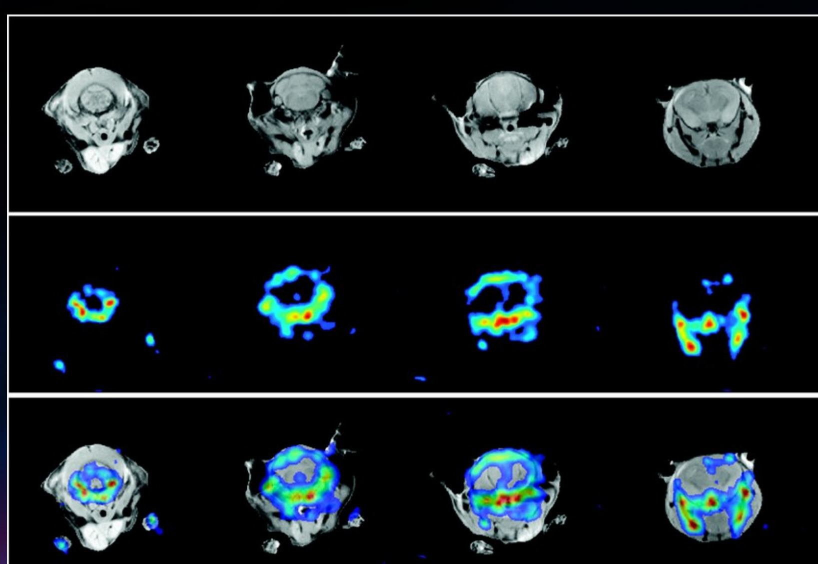

Catana et.al., JNM 47 (12), 2006

UCDAVIS
UNIVERSITY OF CALIFORNIA
cmg

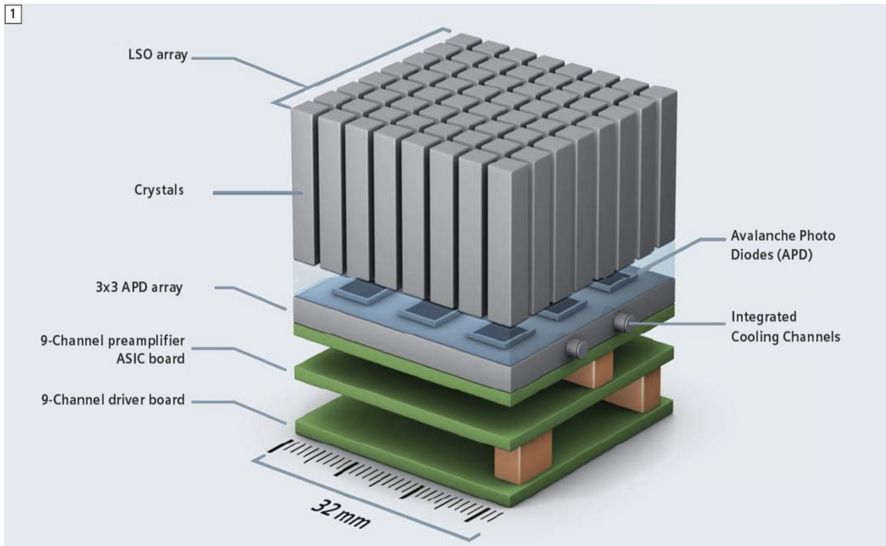

1 Pet detector assembly for mMR. 64 Lutetium Oxyorthosilicate (LSO) crystals form one block that transforms 511 keV gamma quanta into light flashes. Light events in the LSO crystals are detected by a 3x3 array of avalanche photo diodes (ADP). 9-channel preamplifiers and driver boards as well as integrated water cooling completes each detector block. This detector assembly is characterized by its small size, can be designed free of magnetic components, and performs in strong magnetic fields. 56 such blocks form one detector ring, 8 rings form the PET detector assembly in the Biograph mMR that spans a longitudinal field-of-view (FOV) of 25.8 cm.

SIEMENS

MR/PET brain scanner prototype (conceptual design)

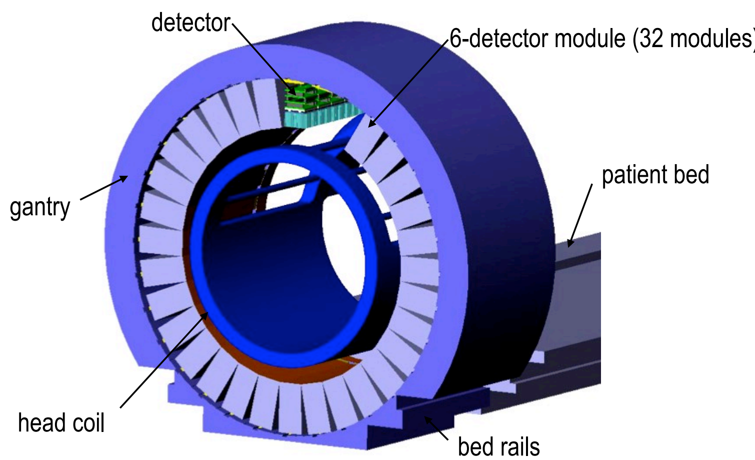

Siemens Medical Solutions that help

SIEMENS

Test Setup

- **Concentric MR and PET**
- **MR:**
  - **CP-TXRX-Head coil inner Diameter 27 cm**
  - **RF Shield iD 36 cm**
- **PET:**
  - **512 LSO crystals in 2 modules**
  - **FOV 3.2 cm**
  - **Imaging by phantom rotation**
- **MR/PET phantom**
  - **1.0 mm - 3.5 mm diameter holes**
  - **Filled with water and 1.25 g $NiSO_4$ / litre and about 50 MBq FDG**

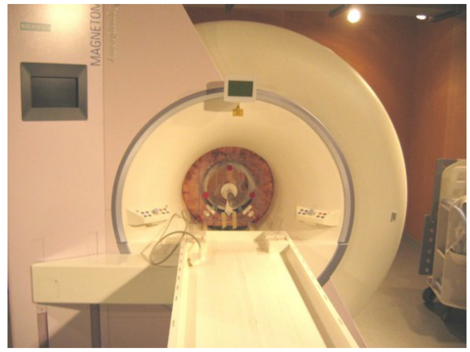

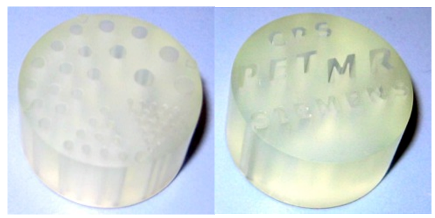

Siemens Medical Solutions that help

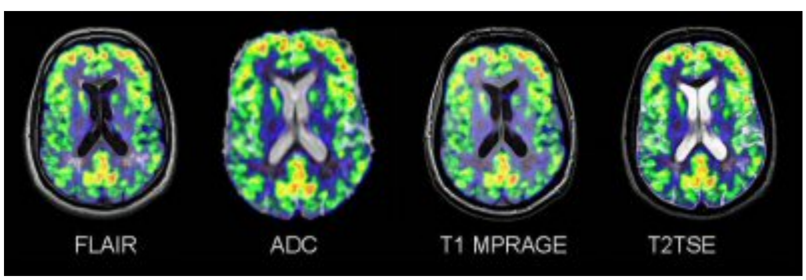

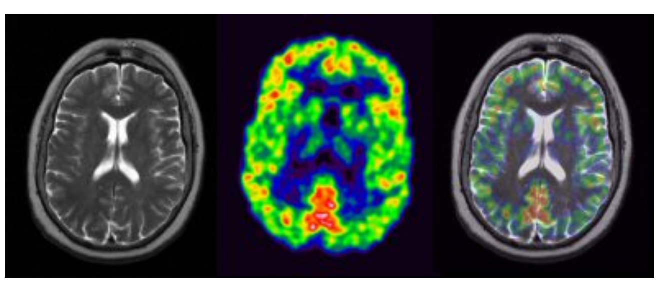

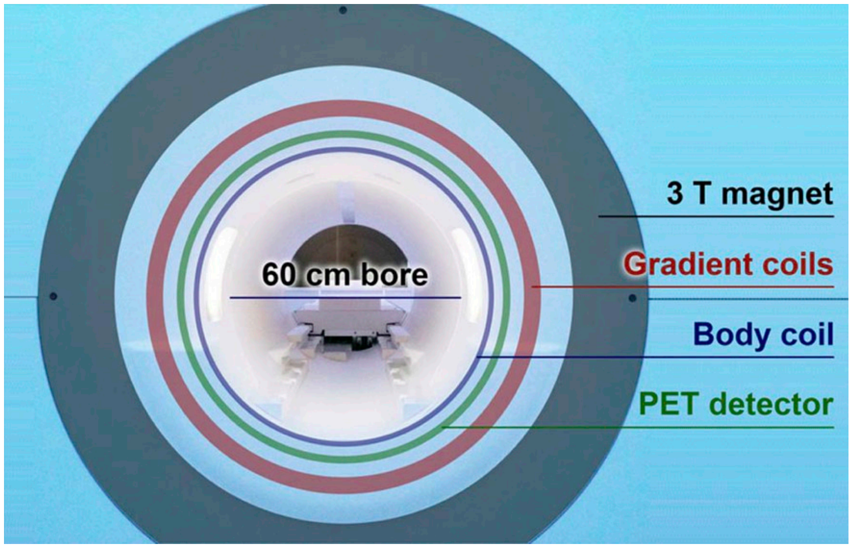

SUPPLEMENTAL FIGURE 1 – Diagram of the Biograph mMR, depicting how the PET detectors are located within the MR coils.

4 The Biograph mMR system installation at the Institute of Medical Physics, University of Erlangen. Both imaging modalities – MR and PET – are fully integrated into one MR/PET hybrid system.

PET-MRI Attenuation Correction

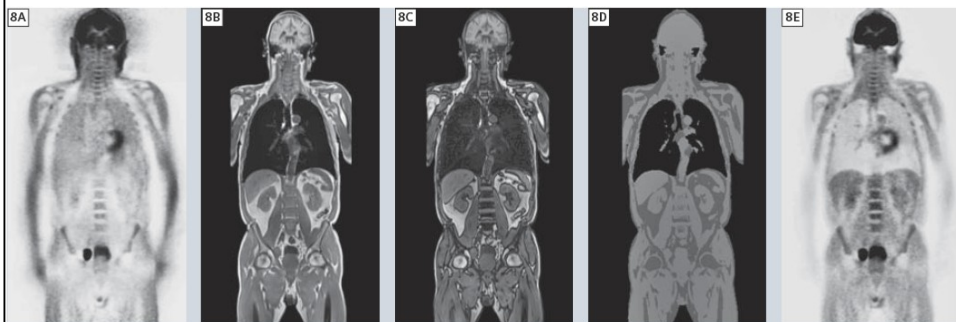

8 Soft-tissue attenuation correction (AC) based on MR imaging. **(A)** Uncorrected whole-body PET scan showing relative activity enhancement in the lungs and on the outer contours of the patient. **(B and C)** Dixon MR sequence providing separate water/fat 'in-phase' and 'opposed phase' images that serve as basis for soft-tissue segmentation. **(D)** Segmented tissue groups (air, fat, muscle, lungs) that can be assigned to 511 keV attenuation maps. **(E)** Resulting attenuation corrected whole-body PET scan of the initial data set **(A)**.

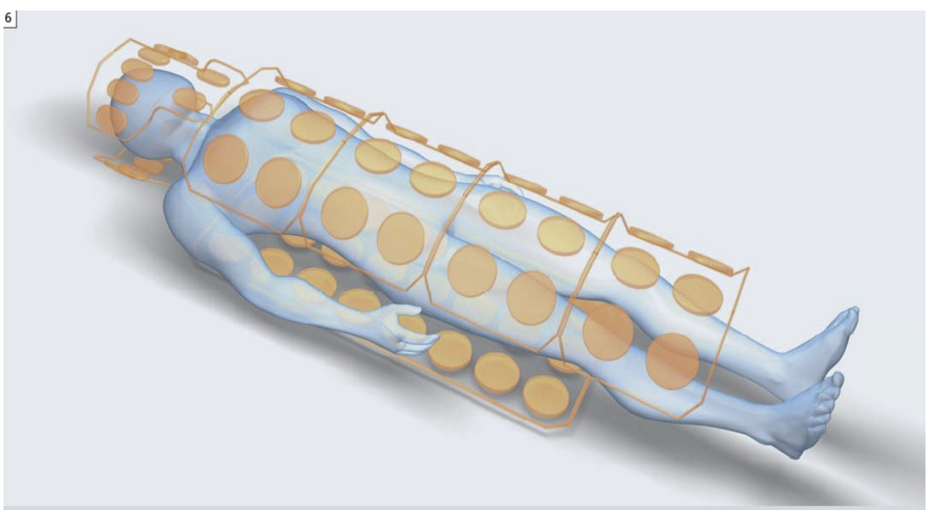

6 The Biograph mMR is equipped with the Tim (Total imaging matrix) RF coil technology consisting of multiple integrated surface coils that cover the patient's body from head to toe with up to 102 RF coil elements connected to 32 RF receivers. This multi-channel phased array RF coil configuration enables parallel imaging and whole-body MR data acquisition with optimized signal-to-noise (SNR) performance. In simultaneous MR/PET hybrid imaging, the surface RF coils are located between the radioactivity emitting patient and the PET detectors. As a consequence, the RF coils should be designed to be as PET-transparent as possible.

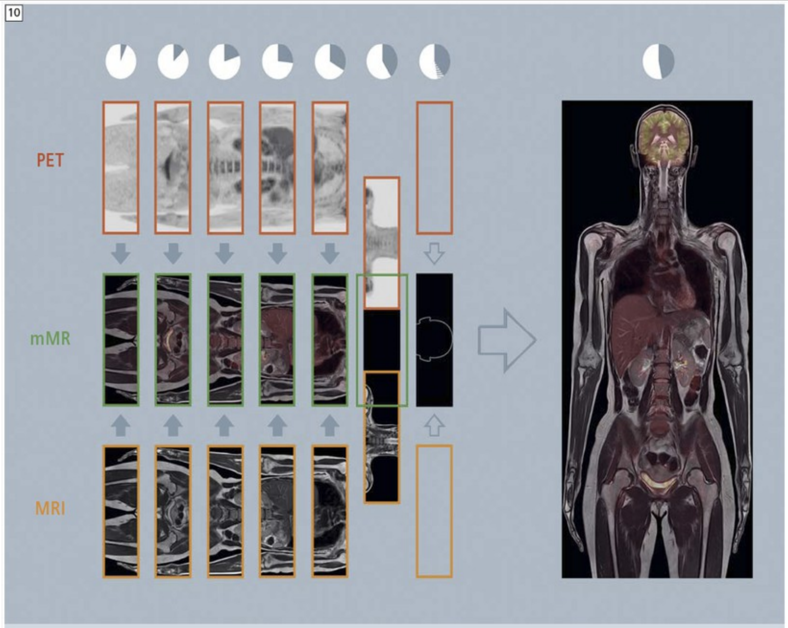

10 MR/PET simultaneous imaging workflow. MR and PET data acquisition is performed simultaneously during a multi-step examination with 6–7 bed positions for whole-body coverage. Depending on the selection of MR imaging sequences, such a whole-body MR/PET hybrid imaging study is regularly completed in about 20–30 minutes.

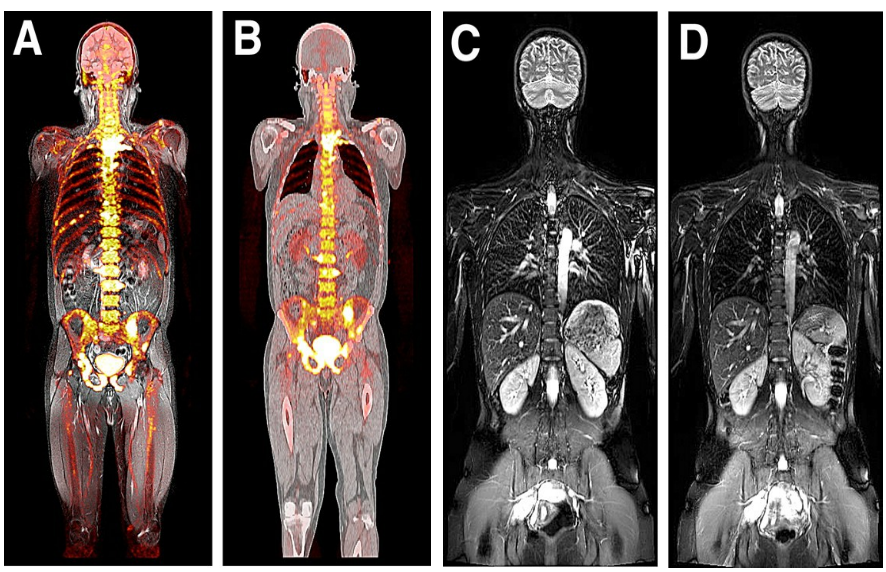

FIGURE 7. mMR PET/MR (A) and Biograph PET/CT (B) fused views of whole-body 18F-fluoride scan of same patient. mMR (C) and Verio (D) T2-weighted coronal views of healthy volunteer.